

Evolution of Photo-induced defects in Ge-doped fiber/preform: influence of the drawing

A. Alessi,^{1,*} S. Girard,² M. Cannas,³ S. Agnello,³ A. Boukenter¹ and Y. Ouerdane¹

¹Laboratoire H. Curien, UMR CNRS 5516, Université Jean Monnet, 18 rue du Pr. Benoît Lauras 42000, Saint-Etienne, France

²CEA, DAM, DIF, F-91297 Arpaçon, France

³Dipartimento di Scienze Fisiche ed Astronomiche, Università di Palermo, I-90123 Palermo, Italy

*antonino.alessi@univ-st-etienne.fr

Abstract: We have studied the generation mechanisms of two different radiation-induced point defects, the Ge(1) and Ge(2) centers, in a germanosilicate fiber and in its original preform. The samples have been investigated before and after X-ray irradiation using the confocal microscopy luminescence and the electron paramagnetic resonance techniques. Our experimental results show the higher radiation sensitivity of the fiber as compared to the preform and suggest a relation between Ge(1) and Ge(2) generation. To explain our data we have used different models, finding that the destruction probability of the Ge(1) and Ge(2) defects is larger in fiber than in preform, whereas the generation one is similar. Finally we found that the higher radiation sensitivity of the fiber at low doses is essentially related to the presence of germanium lone pair center generated by the drawing.

©2011 Optical Society of America

OCIS codes: (060.2310) Fiber optics; (160.2220) Defect-center materials; (300.6370) Spectroscopy, microwave; (350.5610) Radiation; (300.2140) Emission.

References and links

1. G. Pacchioni, L. Skuja, and D. L. Griscom, *Defects in SiO₂ and related dielectrics: Science and Technology*, (Kluwer Academic Publishers, Dordrecht, 2000).
2. C. K. F. Ho, K. Pita, N. Q. Ngo, and C. H. Kam, "Optical functions of (x)GeO₂:(1-x)SiO₂ films determined by multi-sample and multi-angle spectroscopic ellipsometry," *Opt. Express* **13**(3), 1049–1054 (2005).
3. R. Le Parc, B. Champagnon, C. Levelut, V. Martinez, L. David, A. Faivre, I. Flammer, J. L. Hazemann, and J. P. Simon, "Density and concentration fluctuations in SiO₂-GeO₂ optical fiber glass investigated by small angle x-ray scattering," *J. Appl. Phys.* **103**(9), 094917 (2008).
4. A. B. Devine, J. P. Duraud, and E. Dooryhée, *Structure and Imperfections in Amorphous and Crystalline Silicon Dioxide* (Wiley, New York, 2000).
5. J. W. Fleming, "Dispersion in GeO₂-SiO₂ glasses," *Appl. Opt.* **23**(24), 4486–4493 (1984).
6. K. O. Hill, Y. Fujii, D. C. Johnson, and B. S. Kawasaki, "Photosensitivity in optical fiber waveguides: Application to reflection filter fabrication," *Appl. Phys. Lett.* **32**(10), 647–649 (1978).
7. U. Österberg, and W. Margulis, "Dye laser pumped by Nd:YAG laser pulses frequency doubled in a glass optical fiber," *Opt. Lett.* **11**(8), 516–518 (1986).
8. M. Fujimaki, T. Katoh, T. Kasahara, N. Miyazaki, and Y. Ohki, "Paramagnetic centres induced in Ge-doped SiO₂ glass with UV irradiation," *J. Phys. Condens. Matter* **11**(12), 2589–2594 (1999).
9. H. G. Limberger, C. Ban, R. P. Salathé, S. A. Slattery, and D. N. Nikogosyan, "Absence of UV-induced stress in Bragg gratings recorded by high-intensity 264 nm laser pulses in a hydrogenated standard telecom fiber," *Opt. Express* **15**(9), 5610–5615 (2007).
10. H. G. Limberger, P.-Y. Fonjallaz, R. P. Salathé, and F. Cochet, "Compaction- and photoelastic-induced index changes in fiber Bragg gratings," *Appl. Phys. Lett.* **68**(22), 3069–3071 (1996).
11. B. Poumellec, P. Niay, M. Douay, and J. F. Bayon, "The UV-induced refractive index grating in Ge:SiO₂ preforms: additional CW experiments and the macroscopic origin of the change in index," *J. Phys. D Appl. Phys.* **29**(7), 1842–1856 (1996).
12. K. Awazu, H. Kawazoe, and M. Yamane, "Simultaneous generation of optical absorption bands 5.14 and 0.452 eV in 9 SiO₂:GeO₂ glasses heated under H₂ atmosphere," *J. Appl. Phys.* **68**(6), 2713–2718 (1990).
13. L. Skuja, "Isoelectronic series of twofold coordinated Si, Ge, and Sn atoms in glassy SiO₂: a luminescence study," *J. Non-Cryst. Solids* **149**(1-2), 77–95 (1992).
14. V. B. Neustruev, "Colour centres in germanosilicate glass and optical fibres," *J. Phys. Condens. Matter* **6**(35), 6901–6936 (1994).

15. E. J. Friebele, D. L. Griscom, and G. H. Sigel, Jr., "Defect centers in a germanium-doped silica-core optical fiber," *J. Appl. Phys.* **45**(8), 3424–3428 (1974).
16. E. J. Friebele, and D. L. Griscom, "Color center in glass optical fiber waveguides," *Mat. Res. Soc. Symp. Proc.* **61**, 319–331 (1986).
17. M. Fujimaki, T. Kasahara, S. Shimoto, N. Miyazaki, S. Tokuhiro, K. S. Seol, and Y. Ohki, "Structural changes induced by KrF excimer laser photons in H₂-loaded Ge-doped SiO₂ glass," *Phys. Rev. B* **60**(7), 4682–4687 (1999).
18. N. Chiodini, F. Meinardi, F. Morazzoni, A. Paleari, and R. Scotti, "Optical transitions of paramagnetic Ge sites created by x-ray irradiation of oxygen-defect-free Ge-doped SiO₂ by the sol-gel method," *Phys. Rev. B* **60**(4), 2429–2435 (1999).
19. L. Dong, J. L. Archambault, L. Reekie, P. S. Russell, and D. N. Payne, "Photoinduced absorption change in germanosilicate preforms: evidence for the color-center model of photosensitivity," *Appl. Opt.* **34**(18), 3436–3440 (1995).
20. A. Alessi, S. Agnello, S. Grandi, A. Parlato, and F. M. Gelardi, "Refractive index change dependence on Ge(1) defects in γ -irradiated Ge-doped silica," *Phys. Rev. B* **80**(1), 014103 (2009).
21. T. E. Tsai, M. A. Saifi, E. J. Friebele, D. L. Griscom, and U. Osterberg, "Correlation of defect centers with second-harmonic generation in Ge-doped and Ge-P-doped silica-core single-mode fibers," *Opt. Lett.* **14**(18), 1023–1025 (1989).
22. D. L. Griscom, "Trapped-electron centers in pure and doped glassy silica: A review and synthesis," *J. Non-Cryst. Solids* (to be published), doi:10.1016/j.jnoncrysol.2010.11.011.
23. E. J. Friebele, G. H. Sigel, Jr., and D. L. Griscom, "Drawing-induced defect centers in a fused silica core fiber," *Appl. Phys. Lett.* **28**(9), 516–518 (1976).
24. G. Origlio, M. Cannas, S. Girard, R. Boscaino, A. Boukenter, and Y. Ouerdane, "Influence of the drawing process on the defect generation in multistep-index germanium-doped optical fibers," *Opt. Lett.* **34**(15), 2282–2284 (2009).
25. S. Girard, Y. Ouerdane, G. Origlio, C. Marcandella, A. Boukenter, N. Richard, J. Baggio, P. Paillet, M. Cannas, J. Bisutti, J.-P. Meunier, and R. Boscaino, "Radiation effects on Silica-Based preforms and optical fibers—I: Experimental study with canonical samples," *IEEE Trans. Nucl. Sci.* **55**(6), 3473–3482 (2008).
26. A. Alessi, S. Girard, C. Marcandella, M. Cannas, A. Boukenter, and Y. Ouerdane, "Raman investigation of the drawing effects on Ge-doped fibers," *J. Non-Cryst. Solids* **357**(1), 24–27 (2011).
27. S. Agnello, R. Boscaino, M. Cannas, and F. M. Gelardi, "Instantaneous diffusion effect on spin-echo decay: Experimental investigation by spectral selective excitation," *Phys. Rev. B* **64**(17), 174423 (2001).
28. A. Alessi, S. Agnello, F. M. Gelardi, G. Messina, and M. Carpanese, "Influence of Ge doping level on the EPR signal of Ge(1), Ge(2) and E'Ge defects in Ge-doped silica," *J. Non-Cryst. Solids* (to be published), doi:10.1016/j.jnoncrysol.2010.11.108.
29. The difference in positioning the bulk samples (preform and reference sample) and the fiber inside the microwave cavity is the main error source.
30. G. Origlio, S. Girard, M. Cannas, Y. Ouerdane, R. Boscaino, and A. Boukenter, "Paramagnetic germanium-related centers induced by energetic radiation in optical fibers and preforms," *J. Non-Cryst. Solids* **355**(18-21), 1054–1056 (2009).
31. M. Essid, J. Albert, J. L. Brebner, and K. Awazu, "Correlation between oxygen-deficient center concentration and KrF excimer laser induced defects in thermally annealed Ge-doped optical fiber preforms," *J. Non-Cryst. Solids* **246**(1-2), 39–45 (1999).

1. Introduction

Ge doped silica has been studied since many years because this material is used for the realization of several optical devices [1–4]. Historically, Ge doping was used for the production of the fibers because the presence of Ge increases the refractive index of silica [5]. More recently, the interest for this material has increased because the Ge doped fibers have exhibited good photosensitivity [6] and the possibility of inducing, through ionizing radiation, non linear effects [7]. To explain the radiation response of the Ge doped materials, two models have been proposed. The first model, also named color center one, supposes that the radiation releases electrons from the germanium oxygen deficient defects (described in the following) and that these electrons are trapped in other Ge sites [8,9] forming color absorbing point defects. In the second model, the "compaction effects" induced by the irradiation of the materials, are considered to be responsible for the refractive index variations [9–11].

One of the most investigated defects in Ge doped silica is the germanium lone pair center (GLPC) [12], also called twofold-coordinated Ge [13]. It is constituted by a Ge atom, bonded to two oxygen atoms, with two non-bonding electrons forming a lone pair ($=\text{Ge}^{\bullet}$ where $=$ indicates the bonds with two oxygen atoms and \bullet stands for an electron). Previous investigations have shown that this defect is responsible for an optical absorption (OA) band peaked at 5.15 eV ($B_{2\beta}$ band) and for two emission bands peaked at about 4.3 eV (α_E band)

and at 3.2 eV (β band), respectively [13]. In the electronic level scheme reported in [13] the $B_{2\beta}$ band is due to the $S_0 \rightarrow S_1$ transition (S_0 and S_1 being the singlet ground state and the first excited singlet state, respectively), whereas the two emission bands are attributed to the $S_1 \rightarrow S_0$ (α_E band) and to the $T_1 \rightarrow S_0$ transitions (T_1 being the first excited triplet state supplied by an intersystem crossing process from S_1). Finally it is important to remind that an OA band peaked at ~ 3.8 eV (1032 times less intense than the $B_{2\beta}$) has been associated with the $S_0 \rightarrow T_1$ transition [13,14].

The ability of ionizing radiations to generate point defects or to convert them is another well known fact [1,14]. The main radiation-induced defects in Ge-doped silica materials have been reported many years ago by Friebele et al. [15].

Today, after various investigations, they are called Ge(1), Ge(2) and Ge E'. The interest for these defects is related to their links with the radiation induced optical absorption bands even if the attribution of some bands is still debated [14,16–18], to their contribution to photosensitivity [19,20] and non linear effects [21]. The Ge(1) is constituted by an unpaired electron trapped on a tetra-coordinated Ge atom ($=\text{Ge}^{\bullet}=\text{}$) [16,17]. The Ge E' is formed by a threefold coordinated Ge atom having an unpaired electron ($\equiv\text{Ge}^{\bullet}$) [14]. For the Ge(2) two structural models have been proposed. In ref [16], it was proposed that the Ge(2) has a structure similar to Ge(1), in fact they are considered the analogous in glass of the Ge(I) (Ge(2)) and Ge(II) (Ge(1)) in α quartz [22]. At variance, in [17] the authors proposed that the Ge(2) is an ionized GLPC ($=\text{Ge}^{\bullet}$). All these three defects are paramagnetic and can be investigated using the electron paramagnetic resonance (EPR) technique.

Together with the photosensitivity and the structural model studies, a great importance is covered by the comparison between the original starting preforms and the resulting fibers, since from the applicative point of view the control of the fiber features requires the control of the properties of the original preform. Different papers have been dedicated to these arguments: the generation of point defects as a consequence of the drawing has been shown in [23,24], whereas a higher radiation sensitivity of the fibers has been pointed out in [25] and some difference in the glass structure has been reported in [26]. Nevertheless a clear scheme to relate these phenomena is missing. For this reason, in the present investigation we have studied the radiation response of a fiber and its original preform suggesting which of the drawing effects is responsible for the difference in their radiation responses. It is important to underline that the samples' structure has already been studied and the previous study, reported in [26], provides evidence for an increase of the concentration of the three member rings in the fiber, which may indicate a possible densification because of the drawing.

2. Experimental

The studied optical fiber and its original preform have been produced by the iXFiber SAS manufacturer through the Modified Chemical Vapor Deposition process. The fiber, named FGe in the following, was produced from the preform, called PGe, using a drawing speed ~ 40 m/min, a tension ~ 70 g, and a temperature of the furnace of $\sim 1600^\circ\text{C}$. The fiber diameter is about 125 μm , the ratio between the preform and the fiber diameters is 80.4.

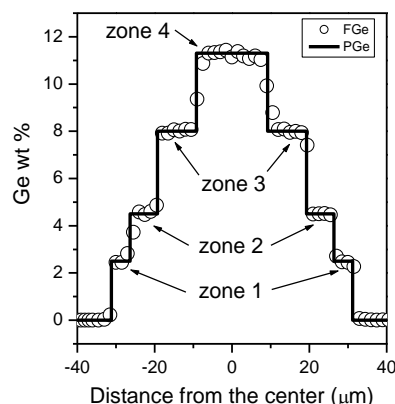


Fig. 1. Ge-doping profile both in FGe fiber (○) and PGe preform (—). The diameter ratio between the preform and the fiber is ~ 80.4 , the values reported on the x-axis have been rescaled by this ratio for the preform.

The preform was designed with the 4-steps radial distribution of Ge doping illustrated in Fig. 1 (the Ge content varies from $\sim 2.5\%$ to $\sim 11\%$ by weight (wt)). In the following, we will refer to the different regions as zone 1 ($\sim 2.5\%$ wt), zone 2 ($\sim 4.5\%$ wt), zone 3 ($\sim 8\%$ wt) and zone 4 ($\sim 11\%$ wt). In the fiber, the dopant profile has been determined by electron microscope analysis, whereas in the preform it is controlled during the production phase. Preform and fiber samples have been X-ray (10 keV) irradiated at room temperature using the ARACOR facility at the French atomic energy center (CEA). The dose rate was 0.02 kGy/s for all the doses, apart for the dose of $5 \cdot 10^{-2}$ kGy that was accumulated by a dose rate of 0.002 kGy/s.

The optical absorption (OA) spectra (range 2.5-6.0 eV) were measured using a single-beam AVANTES S2000 spectrophotometer system, equipped with a D_2 lamp and using a 2048 channels charge coupled device (CCD). We selectively investigated the light transmitted by the different preform zones, using a beam with a diameter lower than 0.5 mm.

We have used the confocal microscopy luminescence (CML) technique to measure both in fiber and preform the radial distribution of GLPC emission at 3.2 eV before and after the irradiations. The CML spectra have been recorded using an Aramis (Jobin-Yvon) spectrometer with a He-Cd ion laser excitation line (energy 3.8 eV, power ~ 0.15 mW on the samples). In addition, this system is equipped with a CCD camera, a microtranslation stage and a 40x objective. The spatial resolution was $\sim 2 \mu\text{m}$. We have also recorded, at room temperature, electron paramagnetic resonance (EPR) spectra using a Bruker EMX-Micro Bay spectrometer working at 9.8 GHz with a magnetic-field modulation frequency of 100 kHz. The total concentrations of the defects have been estimated using as reference the EPR signal of Si E' recorded in a bulk sample of pure silica with a known concentration [27]. Both in fiber and preform the experimental EPR spectra have been decomposed with the Ge(1), Ge(2) and Ge E' reference signals isolated in a sample doped with $\sim 12\%$ of Ge using the different thermal stabilities [28]; the concentrations of the different types of defects have been determined with a relative error of about 20%. The relative error between the concentrations estimated in fiber and preform is about 50% [29]. All types of measurements have been recorded about one month after the irradiation.

3. Results

Figure 2a illustrates the optical absorption spectra recorded in the 11% (zone 4) and 4.5% (zone 2) Ge doped zones of the non-irradiated preform. These spectra clearly evidence the presence of an intense optical absorption band compatible with the optical absorption activity of the GLPC [1,12].

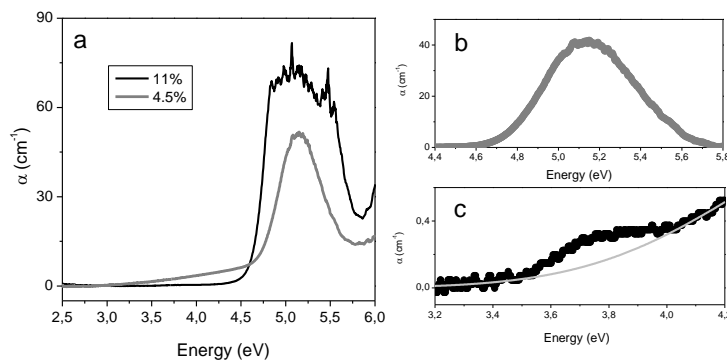


Fig. 2. a) Optical absorption spectra recorded in the ~11% (—) and ~4.5% wt (—) Ge doped zones of the non-irradiated preform; b) optical absorption spectrum of the 4.5% Ge doped zone of the non-irradiated preform after the subtraction of a tangent to the minima of the band (—); c) zoom around 3.8 eV of the optical absorption spectrum recorded in the ~11% Ge doped zone of the non-irradiated preform, the grey curve is a Gaussian tail describing the other OA activities.

Since in the spectrum recorded in the zone 2 the GLPC OA band is not isolated, to estimate the concentration of the GLPC we have subtracted a tangent to the minima of the band (at about 4.6 and 5.8 eV, see Fig. 2b). After this procedure, the concentration, estimated using the Smakula formula (considering a Gaussian line shape for the OA band) [1] and an oscillator strength of ~0.1 [1,14,17,24], is $(1.9 \pm 0.5) \times 10^{18}$ defects/cm³. In zone 4, the GLPC concentration has been estimated using the OA band at ~3.8 eV associated with the $T_1 \rightarrow S_0$ transition [14] and the ratio between the oscillator strength of the $B_{2\beta}$ and that of this transition (~1032 [14]). In particular from the spectrum reported in Fig. 2c after the subtraction of a Gaussian tail describing the other OA activities, we estimated a concentration of $(8.0 \pm 2.6) \times 10^{18}$ defects/cm³.

Figure 3 illustrates the GLPC profiles along the fiber and the preform diameters (the center of the core is located at 0). The two profiles are quite similar, although in the preform the GLPC emission features a decrease followed by a recovery near the center (see inset of Fig. 3), preventing a more definitive conclusion regarding the profile comparison.

Because the absorption coefficient and the thickness (few micron) investigated by CML measurements are low we can consider the absorption and photoluminescence (PL) amplitude at 3.2 eV under excitation at 3.8 eV linearly related, so we can estimate the GLPC concentrations in the different parts of the fiber and perform by comparing the PL amplitude with those recorded in the zones 4 and 2 of the preform. In particular the GLPC concentration at the center of the fiber is $(5.0 \pm 1.6) \times 10^{19}$ defects/cm³. An important result for the following discussion is the value of 6.2 ± 2.2 for the ratio between the GLPC concentrations in fiber and preform. Furthermore, we note that the maximum value of the ratio between GLPC/Ge concentrations is about 0.02 and is observed at the center of the fiber core.

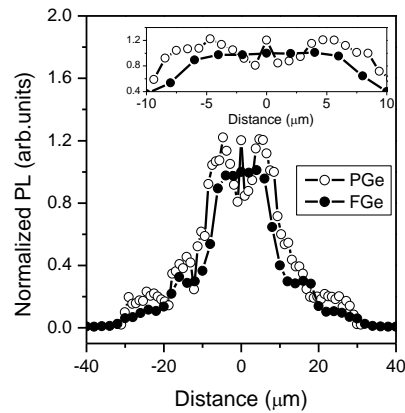


Fig. 3. GLPC profile obtained through CML measurements on the non-irradiated preform (○) and fiber (●) samples as a function of the distance from the core center; in the inset we report the zoom of the CML signal from the core center recorded between -10 and $10 \mu\text{m}$. For the preform data, the distance from the center is rescaled by the ratio between fiber and preform diameters.

After each irradiation dose we have recorded CML measurements on the fiber (see Fig. 4). We remark that the GLPC profile remains unchanged by radiations. We note that the PL amplitude shows a decreasing tendency but that these variations are within the error bar up to 200 kGy . As regards the preform we have recorded CML measurements on the non-irradiated sample and on the sample irradiated at the dose of 200 kGy . The data do not evidence, inside the measurement error, a decrease of the PL luminescence.

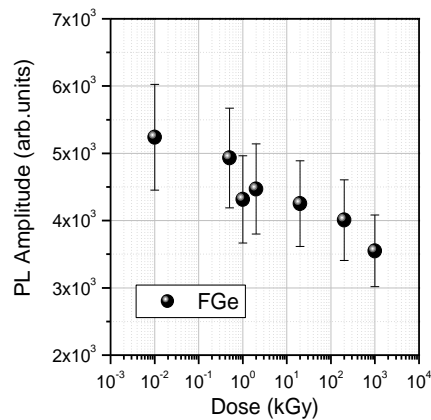


Fig. 4. GLPC related PL amplitude recorded at the center of the fiber core as a function of the irradiation dose expressed in kGray (kGy), the point at 10^{-2} kGy stays for the measurements recorded on the non-irradiated fiber.

Before any irradiation the EPR spectra show that in both FGe and PGe only the signal of the Ge E' is present. The concentration of this type of defects is evaluated to be $\sim 3 \times 10^{16} \text{ defects/cm}^3$ in the FGe and $\sim 3 \times 10^{15} \text{ defects/cm}^3$ in PGe. After irradiation, we observe the generation of other Ge-related paramagnetic point defects as well as the formation of silica intrinsic point defects, such as Si E' ($\equiv \text{Si}^\bullet [1]$). Figure 5a illustrates the EPR spectra recorded at the dose of 20 kGy for FGe and PGe. From these measurements, we can evaluate the induced concentrations of the Ge(1), Ge(2) and Ge E' defects. The spectra are normalized to

their double integrals to compare their line-shapes. From this comparison, we reveal differences in the amplitude of the positive peak at ~346 mT. Basically, this diversity is due to small differences in the relative contributions of the different defects. In particular they are due to the different weights of the Ge(1) and Si E' signals. Regarding possible changes in the line-shapes of the signals that compose the total spectrum, the presence of four signals and the signal to noise ratio of the fiber spectra do not permit definitive conclusions, however the data show that if present such changes have a secondary relevance.

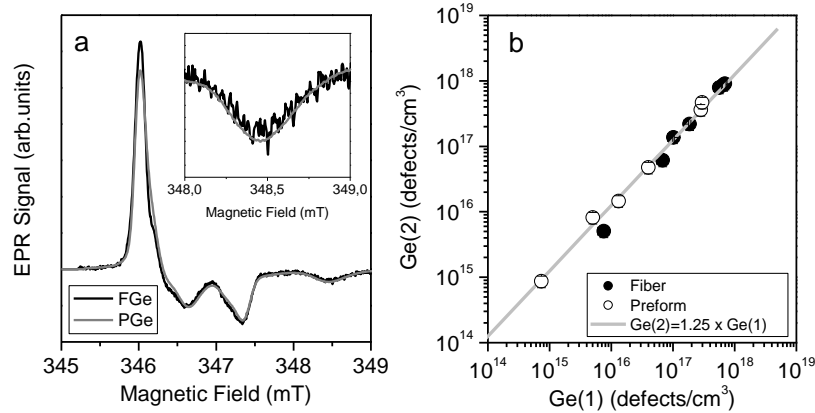
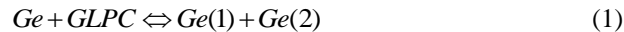


Fig. 5. a) EPR spectra recorded in the fiber (—) and in the preform (—) at the dose of 20 kGy; b) Ge(2) concentration as a function of the Ge(1) concentration in fiber FGe (●) and in preform PGe (○), (—) fit law see the text.

In Fig. 5b, we report the Ge(2) concentration as a function of the Ge(1) concentration. The defects are considered to be principally located in the region delimited by a radius of ~21 μm around the core center (zones 3 and 4). This assumption is justified by the fact that in [30] the absorption spectra show that a 4.5 eV peaked band attributed to Ge(1) [14,16–18] is more evident in zones 3 and 4. For the Ge(2) such hypothesis is supported by the following considerations. If we consider them as ionized GLPC the CML measurements indicate that these regions, having the larger GLPC content, are also the regions in which the Ge(2) formation will be larger. At the same time, if we consider the Ge(2) as a variant of the Ge(1), the higher Ge content in these regions confirms the idea that the Ge(2) concentration will be larger in these zones than in other parts.

4. Mathematical analyses

In the Fig. 5b, we report the fit law $Ge(2)=k \times Ge(1)$ with $k=(1.25 \pm 0.15)$. This value appears sufficiently close to 1 to suppose the following photo-induced process as the main generation mechanism:



where Ge represents a Ge tetra-coordinated atom. In Eq. (1) we also considered the back conversion process as proposed in [8]. The $Ge(1) + Ge(2) \rightarrow Ge + GLPC$ is supported by the data of Fig. 5b, whereas the back conversion mechanism is assumed basing on the data reported in [8]. However, we will also report and comment a data analysis in which this strict relation is not supposed. According to Eq. (1) we can write the following equation for the Ge(1) and Ge(2) generation:

$$\frac{dGe(1,2)}{dx} = c \cdot GLPC(x) \cdot Ge(x) - b \cdot Ge(2) \cdot Ge(1) \quad (2)$$

where x is the dose, $Ge(1,2)$ is the $Ge(1)$ or $Ge(2)$ concentration, $GLPC(x)$ and $Ge(x)$ are the GLPC concentration and the amount of the tetra-coordinated Ge atoms at each dose, c is the generation probability and b the destruction one.

It is important to note that a slight variation of the GLPC concentration in fiber takes place at 1 MGy, when the concentrations of the $Ge(1)$ and $Ge(2)$ have reached a limit value (see Fig. 6). Even if this may suggest the existence of other destruction channels for higher doses, the small amplitude of the change and the dose at which it begins to be observed permit us to approximate the GLPC concentration to be constant in the following model.

As regards the Ge content, it is sufficiently high and the sum of all the Ge related defects is so low that it is possible to assume that at each dose $Ge(x)$ corresponds to the initial Ge content (the Ge atoms not involved in defects are considered to be substitutional in the matrix). So, we can write the Eq. (2) in the following way (similar formulas can be written for the $Ge(2)$):

$$\frac{dGe(1)}{dx} = c \cdot GLPC \cdot Ge - b \cdot (Ge(1))^2 \quad (3)$$

where we have considered that $Ge(1)=Ge(2)$ on the basis of the mechanisms assumed in Eq. (1). Since $Ge(1)=0$ for $x=0$ the solution of Eq. (3) is:

$$Ge(1) = \sqrt{\frac{GLPC \cdot Ge \cdot c}{b}} \cdot \tanh\left[x \cdot \sqrt{GLPC \cdot Ge \cdot c \cdot b}\right] \quad (4)$$

In this way, we can relate the process probabilities to the values obtained by fitting the experimental data with a law $Ge(1,2)=sat \times \tanh(Dsat \times x)$ where sat and $Dsat$ are equal to the saturation value of concentration and the inverse of the saturation dose respectively. Then, we have:

$$\frac{sat^f}{sat^p} = \sqrt{\frac{GLPC^f}{GLPC^p}} \cdot \sqrt{\frac{b^p \cdot c^f}{b^f \cdot c^p}} \quad (5)$$

$$\frac{Dsat^f}{Dsat^p} = \sqrt{\frac{GLPC^f}{GLPC^p}} \cdot \sqrt{\frac{b^f \cdot c^f}{b^p \cdot c^p}} \quad (6)$$

$$\frac{1}{b} = \frac{sat}{Dsat} \quad (7)$$

$$c = sat \cdot Dsat \cdot \frac{1}{Ge \cdot GLPC} \quad (8)$$

It is important to note that we can obtain the destruction probability b using just the result of the data fits, whereas to evaluate the generation probability c we also need the Ge and the GLPC concentrations.

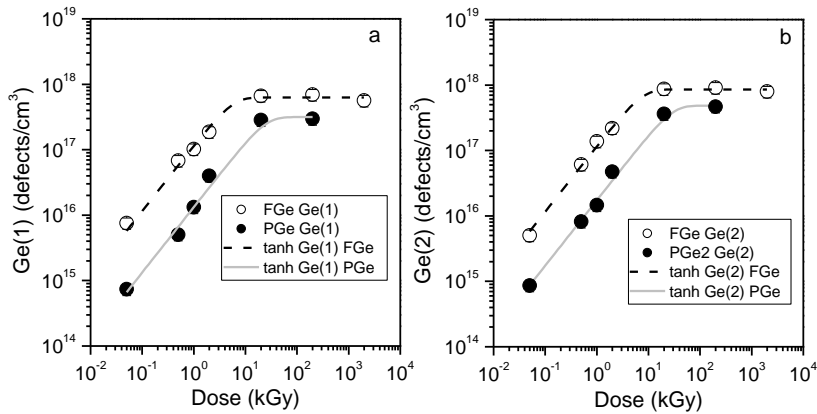


Fig. 6. a) Ge(1) concentration as a function of the dose; b) Ge(2) concentration as a function of the dose. Data of fiber (○) and preform (●), fit of fiber data (---), fit of the preform data (—).

In Fig. 6 we report the experimental concentrations of the Ge(1) and Ge(2) defects obtained for FGe and the PGe at different doses together with the fits obtained using the law $\text{sat} \times \tanh(\text{Dsat} \times x)$.

From the fits of the Ge(1) kinetics, we obtain sat values of $(6.3 \pm 1.6) \times 10^{17}$ defects/cm³, $(3.2 \pm 1.1) \times 10^{17}$ defects/cm³ and Dsat values of $(1.8 \pm 0.5) \times 10^{-1}$ kGy⁻¹ and $(0.40 \pm 0.14) \times 10^{-1}$ kGy⁻¹ for the fiber FGe and the preform PGe, respectively. Similarly from the fits of the Ge(2) kinetics we obtain sat values of $(8.6 \pm 2.2) \times 10^{17}$ defects/cm³ and $(4.9 \pm 1.7) \times 10^{17}$ defects/cm³ and Dsat values of $(1.4 \pm 0.4) \times 10^{-1}$ kGy⁻¹ and $(0.40 \pm 0.14) \times 10^{-1}$ kGy⁻¹ for the fiber FGe and the preform PGe, respectively. It is important to note that in zone 4 the GLPC content is the largest and is one order of magnitude larger than the maximum Ge(2) induced concentration, preventing to evidence the related decrease of the GLPC using the emission or OA spectra. In addition, for the PL measurements, this estimation is limited by the measurement errors; whereas for the OA spectra it is limited by the presence of induced OA bands in the same spectral range of the GLPC OA bands.

The relation between the generation probability and the destruction one in fiber and preform can be evaluated in different ways. In details, it is possible to use the Eq. (5-8), the fits of the data, the square root of the GLPC ratio and the ratio between the concentrations of induced Ge(1) or Ge(2) up to the dose of 2 kGy. In fact, basing on Eq. (4), we note that for low doses ($x \cdot \sqrt{\text{GLPC} \cdot \text{Ge} \cdot c \cdot b} \ll 1$), when the concentrations grow linearly the Ge(1) and the Ge(2) concentrations depend linearly also on the Ge content, the GLPC concentration and the generation probability. In this latter case, the ratio between the concentrations induced in fiber FGe and preform PGe is equal to the ratio $(\text{GLPC}^f \times c^f)/(\text{GLPC}^p \times c^p)$ and its experimental value is about 8. This value is compatible with the ratio between the GLPC concentrations in fiber and preform (~6) evidencing the important role played by the GLPC in the radiation response. In fact, in this case we find $c^f \sim 1.3 c^p$. For the relation between the generation probabilities in fiber and preform, similar results are obtained solving the Eq. (5) and 6, or using Eq. (7) and 8. In these cases we also obtain information regarding the destruction probabilities. Using all these ways we find that $c^f \sim 1.3 c^p$ and $b^f \sim 2.0 b^p$ with an error of about 50%.

Finally, we underline that the Ge(1) and Ge(2) linear dependence on Ge, GLPC concentrations and generation probability is valid also for the photo-process: $\text{Ge} + \text{GLPC} \rightarrow \text{Ge}(1) + \text{Ge}(2)$ that is neglecting the back-conversion process.

As anticipated we can also consider another model in which the Ge(1) and Ge(2) kinetics are not related. In this case, we start from the experimental evidence that for both types of defects it is possible to individuate a saturation value. Applying to the GLPC(x) and Ge(x) the

same considerations above reported, for this second model we can write the following equations in which a generation channel and a destruction one are considered:

$$\frac{dGe(1)}{dx} = q \cdot Ge - r \cdot Ge(1) \quad \frac{dGe(2)}{dx} = s \cdot GLPC - g \cdot Ge(2) \quad (9)$$

$$Ge(1) = \frac{q \cdot Ge}{r} \cdot (1 - e^{-rx}) \quad Ge(2) = \frac{s \cdot GLPC}{g} \cdot (1 - e^{-gx}) \quad (10)$$

$$\frac{sat^f[Ge(1)]}{sat^p[Ge(1)]} = \frac{q^f r^p}{q^p r^f} \quad \frac{sat^f[Ge(2)]}{sat^p[Ge(2)]} = \frac{s^f g^p}{s^p g^f} \cdot \frac{GLPC^f}{GLPC^p} \quad (11)$$

in these equations q and s are the generation probabilities of Ge(1) and Ge(2) defects, whereas r and g are the destruction ones.

Using these equations and fitting the Ge(1) data with the law $sat \times (1 - \exp(-Dsat \times x))$ we obtain that the sat values are of $(6.3 \pm 1.6) \times 10^{17}$ defects/cm³ and $(3.2 \pm 1.1) \times 10^{17}$ defects/cm³ for FGe and PGe, respectively, whereas the $Dsat$ values are $(2.0 \pm 0.5) \times 10^{-1}$ kGy⁻¹ and $(0.40 \pm 0.14) \times 10^{-1}$ kGy⁻¹. Similarly for the Ge(2) we obtain $(8.7 \pm 2.2) \times 10^{17}$ defects/cm³ and $(5.0 \pm 1.7) \times 10^{17}$ defects/cm³ for the sat values of fiber FGe and preform PGe, respectively, and $(1.4 \pm 0.4) \times 10^{-1}$ kGy⁻¹ and $(0.4 \pm 0.14) \times 10^{-1}$ kGy⁻¹ for the $Dsat$ values.

We note that r^f and g^f are ~4 times r^p and g^p (being, $Dsat$ equals to r or g depending on the defect type), whereas from the fits and using the Eq. (10) and 11 we have calculated that q^f is ~9.8 q^p whereas s^f is ~1 s^p .

We have not reported the data of the Ge E', basically since our interest in the present investigation regards the Ge(1) and the Ge(2). However we note that they are a minor contributor up to ~2 MGy. For similar reasons we have not reported the data regarding the concentration Si E' even if it is important to note that the ratio between the concentrations induced in the fiber and in the preform assumes values from 2 to 1 independently from the dose.

5. Discussion

The photo-process of Eq. (1) allows to calculate the generation and destruction probabilities. By using the Eq. (7) and 8 we find that the generation probability c ($\sim 10^{-24}$ kGy⁻¹cm³) is always 5 orders of magnitude lower than the destruction probability b ($\sim 10^{-19}$ kGy⁻¹cm³). These values are useful to explain the experimental fact that the radiation-induced concentrations of Ge(1) and Ge(2) are low even if the concentrations of their precursors are high. In addition, our study indicates the destruction probability b^f is larger than b^p , whereas the generation probabilities c in fiber and the preform are almost similar. Using Eq. (1), we can point out that the differences in Ge(1) and Ge(2) generation between the FGe fiber and the PGe preform are essentially due to the difference in the pre-existing GLPC concentrations and that the ratio between the defects induced in fiber and preform changes with the dose. This aspect is relevant because it shows how the drawing procedure can modify the radiation response of the glass essentially by changing the defect population that for low doses is responsible for the large difference between the FGe fiber and the PGe preform behaviors. At high doses, this large difference is then almost removed since the saturation dose depends on GLPC concentration and because destruction probability is greater in the fiber than in the preform. The structural changes induced by the drawing evidenced in [26] seem to have a lower effect on the radiation response of the fiber, even if their relation with the variation of the destruction probability have to be investigated further for a better-deeper comprehension.

Considering the results obtained supposing the Ge(1) and Ge(2) kinetics as not strictly related we observe that the destruction probabilities of both defect types always appear larger in the fiber than in the preform. This tendency agrees with the here reported first model. As

regards the generation probability of the Ge(1) we found that in fiber it is ~10 times that of the preform; in this model this quantity depends on the electron donor concentration, so that the value of about 10 appears compatible with the ratio between GLPC concentrations in fiber and preform 6 ± 2 . These findings suggest that the GLPC are electron donor and highlight once time again their prevalent role in the radiation sensitivity response. As regards the Ge(1) generation probability, the high Ge content makes negligible the effects of other possible electron trap and leads us to guess that it is very similar in fiber and preform.

In this context we note that in [20] the refractive index changes have been correlated to the Ge(1) and that in [31] they have been related to the starting GLPC content. Our data indicate that these previous investigations are not in contrast since the increase in the GLPC enhances the Ge(1) generation. This means that refractive index changes are strictly related both to Ge(1) and GLPC in all the samples in which other Ge(1) generation channels are negligible.

Finally, we remark that if we consider the Ge(1) and the Ge(2) as two variants of the same defect (an electron trapped on a tetra-coordinated Ge atom) we can apply to both defects the considerations made for the Ge(1) kinetic, when we used the model that does not relate the generation of the Ge(1) and Ge(2). In fact, under this hypothesis the equations that govern the Ge(2) generation became equivalent to those written for the Ge(1). More in detail, in this case we note that using Eq. (9) for the sum of Ge(1) and Ge(2) the fits give the following relations $r^f \sim 4 r^p$ and $q^f \sim 7.8 q^p$, since 7.8 is compatible with the GLPC ratio and since the q implicitly depends on the electron donor concentration the kinetics are compatible with the following process: $\text{Ge} + \text{GLPC} \leftrightarrow \text{GLPC}^+ + (\text{Ge}(1) \text{ or } \text{Ge}(2))$ (the back conversion is supposed). To determine the destruction and the generation probabilities of this photo process, we adapted the method previously reported (see equations from 4 to 8), finding very similar results for the relations between the destruction and the generation probabilities in fiber and preform. As a final remark we underline that with this model the experimental result that Ge(1) and Ge(2) concentrations are almost equal (see Fig. 5b) cannot be clarified.

6. Conclusion

We have investigated by electron paramagnetic resonance and confocal microscopy luminescence measurements the generation processes of the Ge related paramagnetic defects in a fiber and in its original preform. The data have shown the higher radiation sensitivity of the fiber and have indicated that the GLPC are the donor of electrons trapped by the tetra-coordinated Ge atoms. The data indicate that the Ge(1) and the Ge(2) defects are induced in the same concentration, this finding agrees with the previously suggested model in which the Ge(1) is an electron trap center and the Ge(2) is a ionized GLPC. Using a model based on the experimental correlation between the Ge(1) and Ge(2) concentrations, we have found that: (i) the destruction probability of Ge(1) and Ge(2) is about five orders of magnitude higher than the generation one, (ii) the destruction probability in fiber is larger than in preform (iii) the drawing, inducing GLPC in the fiber, increases the radiation sensitivity of the fiber. Moreover, we can suggest that the generation probability of the fiber and preform are similar. For these quantities similar results are found if the Ge(2) is considered a variant of the Ge(1). These results on the kinetics of the Ge(1) and Ge(2) defects formation under irradiation supply relevant information on the basic mechanisms at the origin of the radiation response of Ge doped silica materials.

Acknowledgements

We thank people of the LAMP laboratory (<http://www.fisica.unipa.it/amorphous>) at the Department of Physical and Astronomical Sciences of the University of Palermo for useful discussions and comments.